Spectral Efficiency in Large-Scale MIMO-OFDM Systems with Per-Antenna Power Cost

Derrick Wing Kwan Ng and Robert Schober
Institute for Digital Communications
Universität Erlangen-Nürnberg, Cauerstraße 7, 91058 Erlangen, Germany
Email: {kwan, schober}@lnt.de

***Abstract*—In this paper, resource allocation for multiple-input multiple-output orthogonal frequency division multiplexing (MIMO-OFDM) downlink networks with large numbers of base station antennas is studied. Assuming perfect channel state information at the transmitter, the resource allocation algorithm design is modeled as a non-convex optimization problem which takes into account the joint power consumption of the power amplifiers, antenna unit, and signal processing circuit unit. Subsequently, by exploiting the law of large numbers and dual decomposition, an efficient suboptimal iterative resource allocation algorithm is proposed for maximization of the system capacity (bit/s). In particular, closed-form power allocation and antenna allocation policies are derived in each iteration. Simulation results illustrate that the proposed iterative resource allocation algorithm achieves a close-to-optimal performance in a small number of iterations and unveil a trade-off between system capacity and the number of activated antennas: Activating all antennas may not be a good solution for system capacity maximization when a system with a per antenna power cost is considered.**

I. Introduction

The demand for ubiquitous service coverage and high speed communications has been growing rapidly over the last decade. Multiple-input multiple-output orthogonal frequency division multiplexing (MIMO-OFDM) technology is considered as a viable solution for addressing this issue, as it provides extra degrees of freedom for resource allocation. Specifically, the ergodic capacity of a point-to-point MIMO fading channel increases practically linearly with the minimum of the number of transmitter and receiver antennas [1], [2]. Theoretically, the system performance can be unlimited if the number of antennas at both the transmitter and the receiver is increased. However, the complexity of MIMO receivers limits the performance gains that can be achieved in practical systems, especially for small handheld devices. In order to facilitate the MIMO technology in practice, an alternative form of MIMO has been proposed where a base station (BS) with a large number of antennas serves one single antenna user [3]-[8]. This new paradigm for multiple antenna systems is known as massive MIMO which does not only shift the signal processing burden from the receivers to the BS, but also provides a promising system performance. As a result, massive MIMO system design has recently drawn much attention from both industry and academia [3]-[8].

This work was supported in part by the AvH Professorship Program of the Alexander von Humboldt Foundation.

In [3], high throughput gains were shown to be achievable in both uplink and downlink for a time division duplex (TDD) system with massive MIMO. In [4], the authors derived an achievable downlink data rate for a single-user massive MIMO channel under the constraint of a constant signal envelope per antenna. On the other hand, different receiver signal detection algorithms were studied and channel measurements were carried out for facilitating the implementation of massive MIMO. In [5] and [6], low complexity likelihood ascent search algorithms were proposed for signal detection in large-scale MIMO multicarrier and single carrier systems, receptively. In [7] and [8], channel measurements for massive MIMO systems were reported which revealed the actual potential system performance of large-scale antenna systems. A substantial capacity gain (bit/s/Hz) was observed with massive MIMO compared to single antenna systems in all studies [3]-[8]. Yet, the advantages of massive MIMO do not come for free and the number of antennas cannot be unlimited. In practice, each extra antenna imposes an additional power cost on the power budget due to the associated electronic circuitries [9]. Besides, both the power amplifiers (PAs) and the antenna circuits are sharing the same finite capacity power source at the BS. This joint power consumption model has not been taken into account in the literature so far. Therefore, the results in [3]-[8] which are valid for unlimited numbers of antennas and unlimited power supply, may no longer be applicable for the case of finite numbers of antennas and limited power supply.

In this paper, we address the above issues. In Section II, we introduce the adopted MIMO-OFDM channel. In Section III, we formulate the resource allocation algorithm design as an optimization problem and maximize the system capacity for communication in MIMO-OFDM systems. To this end, an suboptimal iterative algorithm is proposed in Section IV. In Section V, we show that the proposed suboptimal algorithm does not only have a fast convergence, but also achieves a close-to-optimal performance. In Section VI, we conclude with a brief summary of our results.

II. MIMO-OFDM System Model

In this section, after introducing the notation used in this paper, we present the adopted system model.

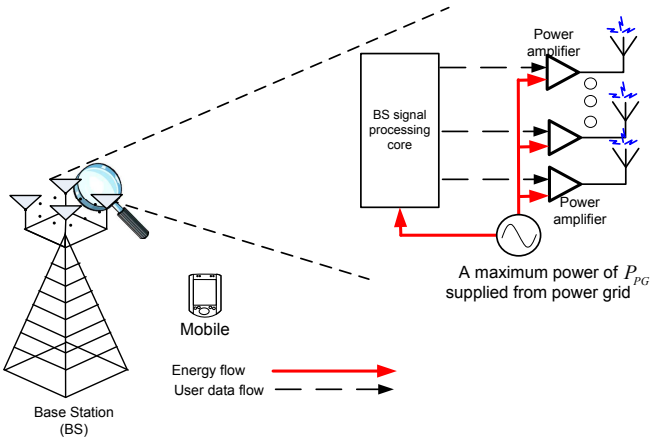

Fig. 1. Illustration of a MIMO-OFDM downlink network and power supply model.

A. Notation

A complex Gaussian random variable with mean μ and variance σ^2 is denoted by $\mathcal{CN}(\mu, \sigma^2)$. $[x]^+ = \max\{0, x\}$. $[x]_b^a = a$, if $x > a$, $[x]_b^a = x$, if $b \leq x \leq a$, $[x]_b^a = b$, if $b > x$. $[x]^+ = \max\{0, x\}$. $|\cdot|$ and $\|\cdot\|$ denote the absolute value of a complex-valued scalar and the Euclidean norm of a vector, respectively. $\mathbb{C}^{N\times M}$ is the space of all $N \times M$ matrices with complex entries and $[\cdot]^T$ denotes the transpose operation.

B. MIMO-OFDM Downlink Channel Model

We consider a MIMO-OFDM system which consists of a BS with multiple antennas and a mobile user equipped with a single antenna, cf. Figure 1. The total bandwidth of the system is $\mathcal{B}$ Hertz and there are n_F subcarriers. Each subcarrier has a bandwidth $W = \mathcal{B}/n_F$ Hertz. We assume a TDD system and the downlink channel gains can be accurately obtained by measuring the uplink channel based on channel reciprocity. The channel impulse response is assumed to be time invariant (slow fading). The downlink received symbol at the user on subcarrier $i \in \{1, \ldots, n_F\}$ is given by

$$y_i = \sqrt{P_i lg}\mathbf{h}_i^T \mathbf{f}_i x_i + z_i, \tag{1}$$

where x_i, P_i, and $\mathbf{f}_i \in \mathbb{C}^{N_{T_i}\times 1}$ are the transmitted symbol, transmitted power, and precoding vector for the link from the BS to the user on subcarrier i, respectively. N_{T_i} is the number of active antennas allocated on subcarrier i for transmission. $\mathbf{h}_i \in \mathbb{C}^{N_{T_i}\times 1}$ is the vector of multipath fading coefficients between the BS and the user. The elements in $\mathbf{h}_i$ are assumed to be independent and identically distributed (i.i.d.). l and g represent the path loss and shadowing between the BS and the user, respectively. z_i is additive white Gaussian noise (AWGN) on subcarrier i with $\mathcal{CN}(0, N_0 W)$, where N_0 is the power spectral density.

III. Resource Allocation Algorithm Design

In this section, we introduce the adopted system performance metric and formulate the corresponding resource allocation problem.

A. Instantaneous Channel Capacity

In this subsection, we define the adopted system performance measure. Given perfect channel state information (CSI) at the receiver, the channel capacity between the BS and the user on subcarrier i with channel bandwidth $W = \mathcal{B}/n_F$ is given by

$$C_i = W \log_2\left(1 + \Gamma_i\right) \text{ and } \Gamma_i = \frac{P_i lg|\mathbf{h}_i^T \mathbf{f}_i|^2}{N_0 W}, \tag{2}$$

where Γ_i is the received signal-to-noise ratio (SNR) at the user on subcarrier i.

The *aggregate system capacity* is defined as a weighted sum of the number of bits per second successfully delivered to the mobile users (bits-per-second) and is given by

$$U(\mathcal{P}, \mathcal{A}) = \sum_{i=1}^{n_F} C_i, \tag{3}$$

where $\mathcal{P}$ and $\mathcal{A}$ are the power allocation policy and the antenna allocation policy, respectively.

B. Power Consumption Model

We model the power dissipation in the system as the sum of three terms [10] which can be expressed as

$$\begin{aligned} U_{TP}(\mathcal{P}, \mathcal{A}) &= U(\mathcal{A}) + U(\mathcal{P}) + P_0 \quad \text{where} \\ U(\mathcal{A}) &= \underbrace{\max_i \{N_{T_i}\} \times P_{A_C}}_{\text{Circuit power consumption of all antennas at the BS}} \quad \text{and} \\ U(\mathcal{P}) &= \underbrace{\sum_{i=1}^{n_F} \varepsilon P_i}_{\text{Power consumption of all power amplifiers at the BS}} . \end{aligned} \tag{4, 5}$$

P_{A_C} is the constant *circuit power consumption per antenna*, which includes the power dissipation of the transmit filter, mixer, frequency synthesizer, and digital-to-analog converter and is independent of the actual transmitted power. In the considered system, we assume that there is a maximum and a minimum number of active antennas, i.e., $N_{\max}$ and $N_{\min}$, at the BS. However, we do not necessarily activate the maximum number of antennas for the sake of efficient communication and the optimal number of active antennas will be found in the next section based on optimization. The physical meaning of the term $\max_i \{N_{T_i}\}$ in (4) is that if an antenna is activated, it consumes power even if it is used only by some of the subcarriers. In other words, the first term in (4) represents the total power consumed by the activated antennas. The second term in (4) denotes the total power consumption in the radio frequency (RF) PAs of the BS. $\varepsilon \geq 1$ is a constant which accounts for the inefficiency in the power amplifier and the power efficiency is defined as $\frac{1}{\varepsilon}$. P_0 is the basic signal processing power consumption which is independent of the number of transmit antennas.

C. Optimization Problem Formulation

The optimal resource allocation policies $(\mathcal{P}^*, \mathcal{A}^*)$ can be obtained by solving

$$\max_{\mathcal{P},\mathcal{A}} \; U(\mathcal{P},\mathcal{A}) \tag{6}$$

$$\text{s.t. C1:} \sum_{i=1}^{n_F} P_i \leq P_{\max},$$

$$\text{C2: } U_{TP}(\mathcal{P},\mathcal{A}) \leq P_{PG}, \quad \text{C3: } P_i \geq 0, \forall i,$$

$$\text{C4: } N_{T_i} \in \{N_{\min}, N_{\min}+1, N_{\min}+2, \ldots, N_{\max}\}, \forall i.$$

$P_{\max}$ in C1 is the maximum transmit power allowance which puts a limit on the transmit spectrum mask to control the amount of out-of-cell interference in the downlink. C2 is imposed to guarantee that the total power consumption of the system is less than the maximum power supply from the power grid, P_{PG}, cf. Figure 1. C3 are the non-negative constraints on the power allocation variables. C4 are the combinatorial constraints on the number of activated antennas.

Note that the above optimization problem formulation can be extended to the case of energy efficiency maximization with imperfect CSI and multiple users, as shown in the related journal paper [11].

IV. Solution of the Optimization Problem

The optimization problem in (6) is a mixed combinatorial and non-convex optimization problem. To obtain an optimal solution, an exhaustive search is needed which is computational infeasible for $N_{T_i}, n_F \gg 1$. To strike a balance between system performance and solution tractability, we transform the problem transformation in the next section.

A. Problem Transformation

We assume that the BS chooses the beamforming vector $\mathbf{f}_i$ to be the eigenvector corresponding to the maximum eigenvalue of $\mathbf{h}_i\mathbf{h}_i^\dagger$, i.e., $\mathbf{f}_i = \frac{\mathbf{h}_i}{\|\mathbf{h}_i\|}$. The adopted beamforming scheme is known as maximum ratio transmission (MRT). Then, we introduce the following proposition by exploiting the properties of large numbers of antennas.

Proposition 1: The asymptotic channel capacity between the BS and the user on subcarrier i for $N_{T_i} \to \infty$ with MRT can be approximated by

$$C_i \overset{(a)}{\approx} W\log_2\Big(1+\Gamma_i\Big) \overset{(b)}{\approx} W\log_2\Big(\Gamma_i\Big) \;\forall i \tag{7}$$

$$\text{where } \Gamma_i = \frac{P_i lg N_{T_i}}{WN_0}. \tag{8}$$

(a) and (b) are due to the law of large numbers and $N_{T_i} \to \infty$, i.e., $\lim_{N_{T_i}\to\infty} \frac{\mathbf{h}_i\mathbf{h}_i^\dagger}{N_{T_i}} = 1$ and $\log_2(1+x) \approx \log_2(x)$ for $x \gg 1$, respectively[1].

It can be observed from (7) that all the subcarriers have the same asymptotic channel gain due to channel hardening [1]. Then, we have the following corollary for the considered resource allocation algorithm design.

[1]In practice, the value of $N_{\min}$ is selected such that the law of large numbers holds.

Corollary 1: In the limiting case of large numbers of antennas with MRT, the resource allocation algorithm is a chunk-based allocation policy. Specifically,

$$N_{T_i}^* = N_T, \; \forall i, \tag{9}$$

$$P_i^* = P, \; \forall i, \tag{10}$$

where P_i^* and $N_{T_i}^*$ denote the optimal power allocation and antenna activation solutions in subcarrier i, respectively. In other words, the BS has no incentive to allocate more resources to a particular subcarrier, since all the subcarriers have the same channel gain for $N_{T_i} \to \infty$.

On the other hand, we need to handle the combinatorial constraint on the antenna activation. We relax constraint C4 such that N_{T_i} can be a real value between $N_{\min}$ and $N_{\max}$ instead of an integer value, i.e., $N_{\min} \leq N_{T_i} \leq N_{\max}, \forall i$. This yields the following relaxed problem:

$$\max_{\mathcal{P},\mathcal{A}} \; \sum_{i=1}^{n_F} W\log_2\Big(\frac{P_i lg N_{T_i}}{WN_0}\Big) \tag{11}$$

$$\text{s.t. C1:} \sum_{i=1}^{n_F} P_i \leq P_{\max}, \quad \text{C2: } U_{TP}(\mathcal{P},\mathcal{A}) \leq P_{PG},$$

$$\text{C3: } P_i \geq 0, \forall i,k, \quad \text{C4: } N_{\min} \leq N_{T_i} \leq N_{\max}, \forall i.$$

Now, we focus on the resource allocation algorithm design for the relaxed problem. Note that the system performance of the relaxed problem will serve as an upper bound of (6). It can be shown that the relaxed optimization problem is jointly concave with respect to (w.r.t.) P_i and N_{T_i}, cf. Appendix. Besides, it can be shown that the relaxed problem satisfies Slater's constraint qualification. As a result, for the relaxed problem, solving the dual problem is equivalent to solving the primal which is known as strong duality [12].

B. Dual Problem Formulation

In this subsection, we solve the power allocation and antenna allocation optimization problem by solving its dual. For this purpose, we first need the Lagrangian function of the primal problem. Upon rearranging terms, the Lagrangian can be written as

$$\begin{aligned}&\mathcal{L}(\lambda,\beta,\mathcal{P},\mathcal{A})\\ &= \sum_{i=1}^{n_F} W\log_2\Big(\frac{P_i lg N_{T_i}}{WN_0}\Big) - \lambda\Big(\sum_{i=1}^{n_F} P_i - P_{\max}\Big)\\ &\quad -\beta\Big(N_{T_i}\times P_{A_C} + \sum_{i=1}^{n_F}\varepsilon P_i + P_0 - P_{PG}\Big).\end{aligned} \tag{12}$$

We note that $\max_i\{N_{T_i}\}$ has been replaced by N_{T_i} in (12) due to Corollary 1. $\lambda \geq 0$ is the Lagrange multiplier corresponding to the maximum transmit power allowance C1. β is the Lagrange multiplier accounting for the power usage from the power grid. On the other hand, boundary constraints C3 and C4 will be absorbed into the Karush-Kuhn-Tucker (KKT) conditions when deriving the optimal resource allocation policies

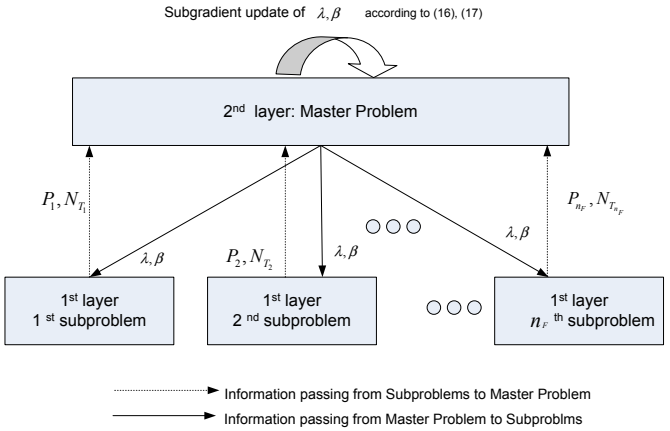

Fig. 2. Illustration of the dual decomposition of a large-scale problem into a two-layer problem.

in the following. Thus, the dual problem is given by

$$\min_{\lambda,\beta\geq 0} \max_{\mathcal{P},\mathcal{A}} \quad \mathcal{L}(\lambda,\beta,\mathcal{P},\mathcal{A}). \tag{13}$$

C. Dual Decomposition

By Lagrange dual decomposition, the dual problem is decomposed into two layers: the first layer consists of n_F subproblems with identical structure; the second layer is the master problem, cf. Figure 2. Then, the dual problem can be solved iteratively, where in each iteration the transmitter solves the subproblem by using the KKT conditions for a fixed set of Lagrange multipliers, and the master problem is solved using the gradient method.

1) Subproblem Solution: Using standard optimization techniques and the KKT conditions, the closed-form resource allocation policies in subcarrier i are obtained as:

$$P_i^* = P = \left[\frac{\mathcal{B}}{\ln(2)(\lambda+\beta\varepsilon)}\right]^+, \quad \forall i, \tag{14}$$

$$N_{T_i}^* = N_T = \left[\frac{\mathcal{W}}{\ln(2)P_{A_C}\beta}\right]_{N_{\min}}^{N_{\max}}, \forall i. \tag{15}$$

The resource allocation solution in (14) and (15) can be interpreted as a water-filling scheme. It can be observed that the BS does not always activate all the antennas for maximization of the system capacity which is limited by the total power supply P_{PG} via β, cf. (15). Note that since the solution of the n_F subproblems are identical, the complexity in solving the n_F subproblems can be reduced by a factor of n_F by just focusing on one subproblem.

2) Master Problem Solution: The dual function is differentiable and, hence, the gradient method can be used to solve the second layer master problem in (13) which leads to

$$\lambda(m+1) = \Big[\lambda(m) - \xi_1(m) \times (P_{\max} - n_F P)\Big]^+, \tag{16}$$

$$\beta(m+1) = \Big[\beta(m) - \xi_2(m) \times (P_{PG} - N_T \times P_{A_C} - n_F\varepsilon P - P_0)\Big]^+, \tag{17}$$

where index $m \geq 0$ is the iteration index and $\xi_u(m)$, $u \in \{1,2\}$, are positive step sizes. Since the relaxed problem is concave in nature, it is guaranteed that the iteration between master problem and subproblems converges to the optimal solution of (13), if the chosen step sizes satisfy the infinite travel condition [12], [13]. Then, the updated Lagrange multipliers in (16), (17) are used for solving the subproblems in (13) via updating the resource allocation policies.

Note that the resource allocation solutions obtained in (14) and (15) are optimal w.r.t. the relaxed problem in (11) for $N_{T_i} \gg 1$.

V. Simulation Results

In this section, we study the performance of two algorithms via simulation. The first algorithm achieves the upper bound performance of (6) by solving the relaxed problem in (11) as outlined in Section III-C. For the second algorithm, we apply a floor function $\lfloor\cdot\rfloor$ to the antenna allocation solution in (15), i.e., $N_{T_i} = \lfloor N_{T_i}^* \rfloor$, which achieves a suboptimal performance w.r.t. the original problem formulation in (6). For the system setting, there are $n_F = 128$ subcarriers with carrier center frequency 2.5 GHz and a total system bandwidth of $\mathcal{B} = 5$ MHz. We assume a noise power of $N_0 W = -118$ dBm in each subcarrier. The desired user is located at a distance of $d_0 = 500$ m from the BS. Log-normal shadowing with a standard deviation of 8 dB is assumed. The multipath fading coefficients of the BS-to-user link are modeled as i.i.d. Rayleigh random variables with unit variances. The average system capacity is obtained by assuming capacity-achieving codes and counting the amount of data which is successfully decoded by the user averaged over both shadowing and multipath fading. We assume a static circuit power consumption of $P_0 = 40$ dBm [14]. The additional power dissipation incurred by each extra antenna for transmission is $P_{A_C} = 30$ dBm [9]. On the other hand, we assume a power efficiency of 40% in the RF PA, i.e., $\varepsilon = \frac{1}{0.4} = 2.5$. The maximum and minimum numbers of active antennas are set to $N_{\max} = 500$ and $N_{\min} = 10$, respectively.

A. Convergence of Iterative Algorithm

Figure 3 illustrates the evolution of the proposed iterative algorithm for different values of maximum transmit power allowance, $P_{\max}$, and maximum power supply, P_{PG}. The results in Figure 3 were averaged over 100000 independent adaptation processes where each adaptation process involves different realizations of the shadowing and the multipath fading. It can be observed that the iterative algorithm converges to values close to the upper bound performance within 4 iterations for all considered cases. In other words, a close-to-optimal system capacity can be achieved within a few iterations on average.

In the following case studies, we focus on the suboptimal algorithm and set the number of iterations in the algorithm to 5.

B. Average Capacity versus Maximum Power Supply

Figure 4 illustrates the average system capacity (bit/s/Hz) versus the maximum power supply from the power grid, P_{PG},

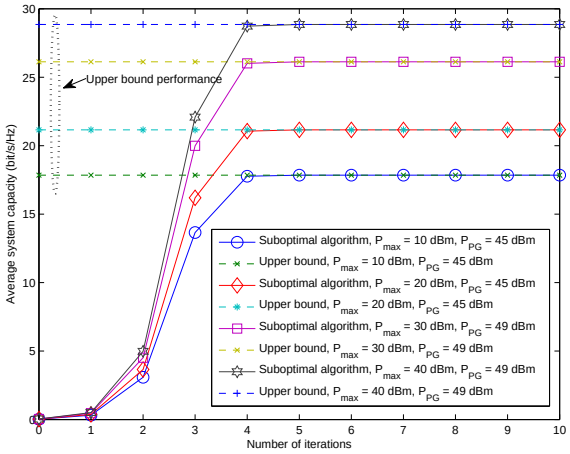

Fig. 3. Average system capacity (bit/s/Hz) versus number of iterations with different maximum powers supplied by the power grid, P_{PG}, and different values of maximum transmit power allowance, $P_{\max}$. The dashed lines represent an upper bound on maximum average system capacity for different cases.

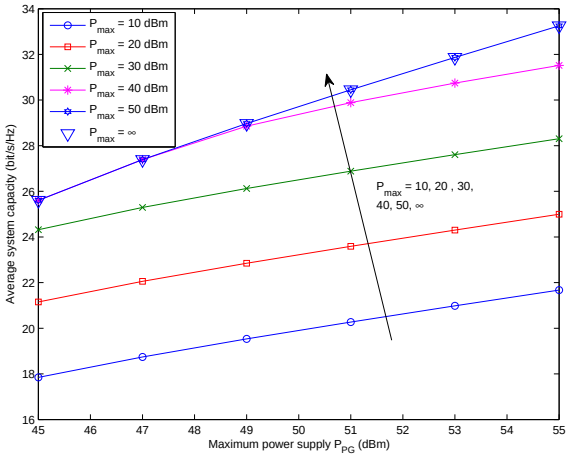

Fig. 4. Average system capacity (bit/s/Hz) versus the maximum power supplied by the power grid, P_{PG}, for different values of maximum transmit power allowance, $P_{\max}$.

for the proposed suboptimal algorithm. Different values of maximum transmit power allowance, $P_{\max}$, are considered. It can be observed that the average system capacity increases for increasing amount of power supplied by the power grid, since more power is available at the BS for resource allocation. On the other hand, the system performance also benefits from increasing values of $P_{\max}$. Indeed, from an optimization theory point of view, a larger value of $P_{\max}$ spans a larger feasible solution set which results in a possibly higher objective value. However, there is a diminishing return in performance as $P_{\max}$ increases, especially in the low power supply regime, i.e., $P_{PG} < 49$ dBm. This is because the system performance is limited by the small amount of power P_{PG} supplied by the power grid, instead of $P_{\max}$.

C. Average Number of Activated Antennas and Power Consumption versus Maximum Power Supply

Figure 5 depicts the average number of activated antennas versus maximum power supply, P_{PG}, for the proposed suboptimal algorithm. The number of activated antennas increases rapidly w.r.t. the an increasing P_{PG} due to a larger amount of available power at the BS. However, the curves in Figure 5 have different slopes for different values of $P_{\max}$. In particular, the number of activated antennas increases with P_{PG} much faster for a small value of $P_{\max}$ than for a large value of $P_{\max}$. This is because for a small value of $P_{\max}$, the system performance is always limited by the amount of power radiated in the RF. As a result, the BS tends to activate more antennas for increasing the antenna array gain. On the other hand, when the value of $P_{\max}$ increases, the BS will allocate more power to the RF and decrease the number of activated antennas. Counterintuitively, the BS does not activate all antennas for maximizing the average system capacity, when both the PAs and the antennas are consuming powers from the same power source.

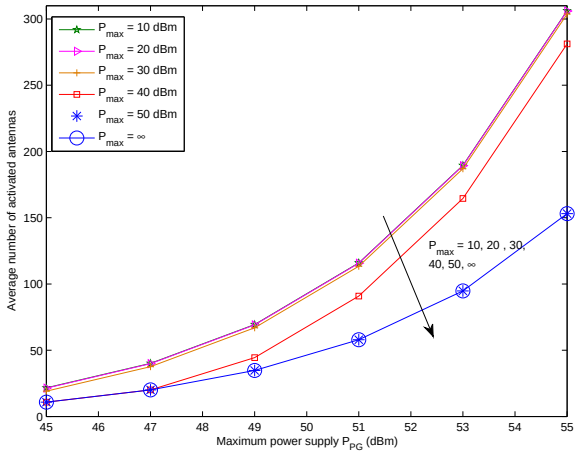

Fig. 5. Average number of activated antennas versus the maximum power supplied by the power grid, P_{PG}, for different values of maximum transmit power allowance, $P_{\max}$.

Figure 6 depicts the power consumption ratio between the PAs and antennas circuits, i.e., $\frac{\mathcal{U}(\mathcal{P})}{\mathcal{U}(\mathcal{A})}$, versus maximum power supply, P_{PG}, for the proposed suboptimal algorithm. We can see that for a small value of $P_{\max}$, the BS spends more power on activating antennas when P_{PG} increases. This is because more antennas will be activated to enhance the system capacity when the radiated power in the RF reaches $P_{\max}$. This observation coincides with the results in Figure 5. On the other hand, when $P_{\max}$ increases, the power consumption of both the PAs and the antenna activation approach the same value for maximizing the system capacity. Indeed, the BS does not have a higher preference for spending more power in the PAs than for activating more antennas, or vice versa, when the constraints on both $P_{\max}$ and $N_{\max}$ in (6) become less

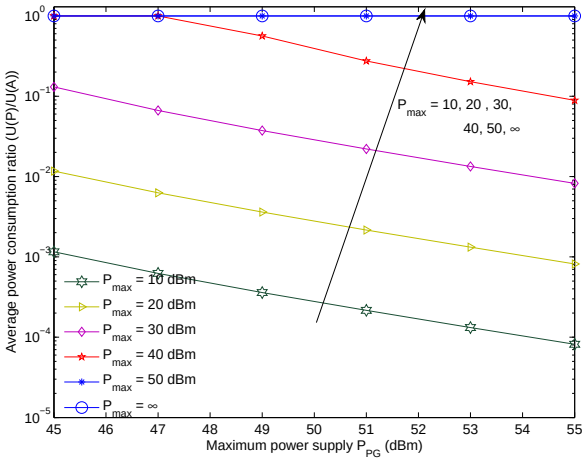

Fig. 6. Average power consumption ratio between PAs and antennas circuits, i.e., $\frac{\mathcal{U}(\mathcal{P})}{\mathcal{U}(\mathcal{A})}$, versus the maximum power supplied by the power grid, P_{PG}, for different values of maximum transmit power allowance, $P_{\max}$.

stringent. On the contrary, the BS tries to maintain a balance between the power consumption in the PAs and the antenna circuits. As a result, activating all available antennas may not be a good solution for system capacity maximization, since the power consumptions in the antennas and PAs should be balanced.

VI. Conclusion

In this paper, we formulated the resource allocation algorithm design for MIMO-OFDM networks with large numbers of BS antennas as a non-convex optimization problem, where a joint power consumption model for the antennas, power amplifiers, and signal processing circuit unit was taken into consideration. An efficient iterative resource allocation algorithm with optimized power allocation and antenna allocation policies was proposed. Our simulation results did not only show that the proposed algorithm converges within a small number of iterations, but also unveiled the trade-off between maximum system capacity and the number of activated antennas.

Appendix - Proof of Concavity of Relaxed Problem

Let $\mathbf{H}(C_i)$ and λ_1, λ_2 be the Hessian matrix of function C_i and the eigenvalues of $\mathbf{H}(C_i)$, respectively. The Hessian matrix of function C_i can be expressed as

$$\mathbf{H}(C_i) = \begin{bmatrix} \frac{-W}{P_i^2 \ln(2)} & 0 \\ 0 & \frac{-W}{N_{T_i}^2 \ln(2)} \end{bmatrix}. \quad (18)$$

Therefore, the corresponding eigenvalues of the Hessian matrix are given by

$$\lambda_1 = \frac{-W}{P_i^2 \ln(2)} \quad \text{and} \quad \lambda_2 = \frac{-W}{N_{T_i}^2 \ln(2)}. \quad (19)$$

Since $\lambda_r \leq 0$, $r = \{1, 2\}$, so $\mathbf{H}(C_i)$ is a negative semi-definite matrix and C_i is jointly concave w.r.t. P_i and N_{T_i}. The summation of C_i over i preserves the concavity of the objective function in [12]. On the other hand, constraints C1-C5 in (11) with relaxed N_{T_i} span a convex feasible set and thus the transformed problem is a concave optimization problem.

References

[1] D. Tse and P. Viswanath, *Fundamentals of Wireless Communication*, 1st ed. Cambridge University Pres, 2005.

[2] A. Goldsmith, *Wireless Communications*. Cambridge University Press, 2005.

[3] T. Marzetta, "Noncooperative Cellular Wireless with Unlimited Numbers of Base Station Antennas," *IEEE Trans. Wireless Commun.*, vol. 9, pp. 3590–3600, Nov. 2010.

[4] S. K. Mohammed and E. G. Larsson, "Single-User Beamforming in Large-Scale MISO Systems with Per-Antenna Constant-Envelope Constraints: The Doughnut Channel," *IEEE Trans. Wireless Commun.*, vol. PP, pp. 1–14, 2012.

[5] K. Vishnu Vardhan, S. Mohammed, A. Chockalingam, and B. Sundar Rajan, "A Low-Complexity Detector for Large MIMO Systems and Multicarrier CDMA Systems," *IEEE J. Select. Areas Commun.*, vol. 26, pp. 473 –485, Apr. 2008.

[6] P. Li and R. Murch, "Multiple Output Selection-LAS Algorithm in Large MIMO Systems," *IEEE Commun. Lett.*, vol. 14, pp. 399–401, May 2010.

[7] X. Gao, O. Edfors, F. Rusek, and F. Tufvesson, "Linear Pre-Coding Performance in Measured Very-Large MIMO Channels," in *Proc. IEEE Veh. Techn. Conf.*, Sep. 2011, pp. 1 –5.

[8] S. Payami and F. Tufvesson, "Channel measurements and analysis for very large array systems at 2.6 ghz," in *2012 6th European Conf. on Antennas and Propag. (EUCAP)*, Mar. 2012, pp. 433 –437.

[9] R. Kumar and J. Gurugubelli, "How Green the LTE Technology Can be?" in *Intern. Conf. on Wireless Commun., Veh. Techn., Inform. Theory and Aerosp. Electron. Syst. Techn.*, Mar. 2011.

[10] R. Prabhu and B. Daneshrad, "Energy-Efficient Power Loading for a MIMO-SVD System and its Performance in Flat Fading," in *Proc. IEEE Global Telecommun. Conf.*, Dec. 2010, pp. 1–5.

[11] D. Ng, E. Lo, and R. Schober, "Energy-Efficient Resource Allocation in OFDMA Systems with Large Numbers of Base Station Antennas," *IEEE Trans. Wireless Commun.*, vol. 11, pp. 3292 –3304, Sep. 2012.

[12] S. Boyd and L. Vandenberghe, *Convex Optimization*. Cambridge University Press, 2004.

[13] S. Boyd, L. Xiao, and A. Mutapcic, "Subgradient Methods," *Notes for EE392o Stanford University Autumn*, 2003-2004.

[14] O. Arnold, F. Richter, G. Fettweis, and O. Blume, "Power Consumption Modeling of Different Base Station Types in Heterogeneous Cellular Networks," in *Proc. Future Network and Mobile Summit*, 2010, pp. 1–8.